PORT SAID ENGINEERING RESEARCH JOURNAL

Faculty of Engineering - Port Said University
Volume (27) No. 4 pp: 124-133

Improving the Structural Integrity of Composite Blades in Vertical Axis Wind Turbines: A Parametric Study Employing the Finite Element Method

*Rasha M. Soliman[1], Shaban M. Abdo[2], Aly El Domiaty[3], Mohamed Lotfy[4, *]*

[1, 2] Production and Mechanical Design department, Faculty of Engineering, Port Said University, Port Said, Egypt, email: rm.soliman@yahoo.com, smiabdou@hotmail.com

[3] Mechanical Engineering department, Faculty of Engineering, Suez Canal University, Ismailia, Egypt, email: alyeldomiaty@yahoo.com

[4] Aerospace Engineering department, Faculty of Engineering, Cairo University, Giza, Egypt. email: lotfytaha@cu.edu.eg

**Corresponding author, DOI: 10.21608/PSERJ.2023.255114.1301*

Received 12-12-2023
Revised 18-12-2023
Accepted 31-12-2023

ABSTRACT

The objective of this work is to conduct a stress analysis of an H-rotor vertical axis wind turbine (VAWT) blade under aerodynamic loads. The rotor blade is designed based on the maximum deflection and bending stresses at extreme loading conditions, specifically the maximum radial force acting on the blade. The impact of the tip speed ratio and blade pitch angle on the bending stress of the H-rotor VAWT is presented. Analytical beam theories are used to determine the maximum deformation and bending stress, which are then verified numerically using the finite element method (FEM) with ANSYS software. The blade is composed of S-2 fiberglass/Epoxy composite material. The stress analysis is performed on both a solid cross-section blade and a hollow blade with varying wall thickness. A comparison is made between the S-2 fiberglass/Epoxy and carbon fiber/Epoxy composites, revealing that carbon fiber composites induce greater deflection in the rotor blade compared to S-2 fiberglass blades. Additionally, it is concluded that the tip speed ratio directly affects both the bending stress and total deflection of the blade.

Keywords: Renewable Energy, VAWT, Tip Speed Ratio, Finite Element, Composite blades.

1 INTRODUCTION

Over the past few decades, a wide array of wind turbine design configurations has been developed. These designs are classified into two main groups, Horizontal Axis Wind Turbine (HAWT) and Vertical Axis Wind Turbine (VAWT), based on their aerodynamic and mechanical properties, blade shape, rotation direction, and rotor shape. The focus of this study is on the straight-bladed H-rotor VAWT, which offers simplicity in construction and several advantages over other wind turbine types. Notably, VAWTs can generate power independently of wind direction, eliminating the need for a yaw control device. Furthermore, VAWTs operate at slower rotational speeds than HAWTs, resulting in lower noise levels. VAWTs also offer cost advantages in terms of production and maintenance costs [1]. The primary load acting on the wind turbine blade is the radial force, which comprises the normal force and centrifugal force. The radial force induces bending stresses in the blade [2-5]. The centrifugal force has a significant influence on the radial force, as well as the resulting stresses and maximum deflection of the blade. The blade mass strongly affects the maximum values of the centrifugal force.

Hand and Cashman [6] provide a historical overview of the lift-type vertical axis wind turbine (VAWT) from its early development in the 1930s to its limited engineering progress in the 1990s. They highlight the recent Renaissance of VAWT in the offshore floating wind turbine industry, discussing the latest developments and attempts to commercialize this technology. Hameed and Afak [7] conducted a design study on a straight symmetrical blade for a small-scale VAWT. They employed beam theories for analytical modeling and the finite element method for numerical modeling. The design was analyzed under extreme wind conditions to determine the maximum deflection and bending stresses. The study concluded that optimizing the blade wall thickness can reduce the weight of the blade while maintaining the maximum stresses and deflection within acceptable limits. Nezzar et al. [8] conducted a Finite Element Analysis to assess the design feasibility of a small-scale aluminum blade for a VAWT. The stress analysis, considering environmental loads such as gravity, wind, and centrifugal forces, confirmed the stability and favorable mechanical properties of the blade structure based on maximum von Mises stresses and deflections. Rahman et al. [9] utilized finite element static stress analysis to design an efficient and stable VAWT using different materials. The H-rotor turbine model was tested with two different airfoils, NACA 0012 and NACA 0714. Stainless steel exhibited the least deformation for all airfoils, while aluminum experienced slightly more deformation, and PVC showed the highest amount of deformation. Liu and Xiao [10] designed a three-dimensional VAWT with H-type blades and focused on analyzing the blade structure features related to bending and twist deflection. Two different blade materials and two strut locations were investigated, revealing an uneven distribution of structural stress along the blade with a high-stress regime near the strut location. Yutaka et al. [11] used computational fluid dynamics (CFD) to study the effects of different arm designs on the performance of a small-sized straight-bladed vertical axis wind turbine (VAWT). They found that the pressure-based tangential force of the arms increased near the connection with the blades, while the friction-based tangential force of the blades decreased around the connection with the arms. The resistance torque added by the arms was larger than the added resistance torque of the blades, except in the case of an airfoil arm rotor. Hand et al. Yanzhao et al. [12] investigated the impact of blade pitch angles on a straight-bladed VAWT using wind tunnel experiments and CFD simulations. The study found that the blade pitch angle had minimal influence on the aerodynamic characteristics of the Straight-bladed VAWT. Hand et al. [13] examined the structural analysis of a VAWT blade under a critical load case using an analytical model and FE model. They found that a composite blade design effectively resisted flap-wise loading and kept material strains within acceptable limits. The analytical approach was shown to be a reliable and efficient method for computing the strain distribution in composite blades, yielding comparable results to the FE model. Arora et al. [14] conducted a study on the optimization and structural behavior of vertical axis wind turbine (VAWT) blades in the offshore environment. They performed probabilistic analysis of wind speed data and estimated wind-induced pressure using CFD simulations. The study also involved structural analysis of hollow composite blades to ensure stresses and deflections are within allowable limits, aiming for an improved and efficient design of VAWTs in Indian offshore environments.

Selecting a low-density material with high mechanical properties is crucial for optimizing wind turbine lifespan and performance. S-2 fiberglass/Epoxy composites offer numerous advantages that make them suitable for wind turbine blade design [15].

In the present research, the stress analysis of the blade is conducted using the finite element method. The blade is constructed with a honeycomb sandwich structure to enhance stress endurance. The analytical stress calculations using beam theories are used to verify the results.

2 ANALYTICAL METHOD

2.1 Wind Turbine Design Parameters

The aerodynamic blade loads and performance calculations for the H-rotor straight-bladed turbine were performed by Rasha et al. [15] and Rasha [16]. Table (1) presents the parameters selected for the basic design of the three-bladed H-rotor VAWT.

Table 1. Three-bladed H-rotor VAWT Design parameters

Parameter	Value
Blade airfoil	NACA0021
Rotor radius	1 m
Blade chord	0.2 m
Rotor Length	2 m
Free stream velocity	5 m/sec
Angular velocity	20 rad/sec
Tip speed ratio	3, 4, 5, 6
Pitch angle	0^o

2.2 Bending Stress

The importance of struts in VAWT design was emphasized by Paraschivoiu [17]. Struts ensure blade stability during rotation, transfer torque to the central column, reduce mean and fatigue stresses in the blades, and affect the rotor's natural frequencies. Supporting struts must possess sufficient strength to carry weight, inertial and aerodynamic loads, and exhibit stiffness in flexure and torsion to prevent excessive static and dynamic deflections [7].

The blades of the H-rotor VAWT can be supported with the horizontal struts in three different ways: a) simple support, b) overhang support and, c) cantilever support. For small capacity H-rotor VAWT with high blade bending moments due to centripetal acceleration, either simple or overhang supports that utilizes two struts per blade are preferable [18]. Furthermore, long blades generally require two points of support for structural reasons [19].

The beam theories are applied to determine the location of the Bessel points and by assuming the blade as a simply supported beam with a uniformly distributed load. The maximum bending moments will occur at the supports and at the center [16]. The calculated optimal distance for the supports is to be placed at a distance 20.7% of the total blade length from both ends. The bending stress acting on the solid blades is given by Perkins and Cromack [20].

3 FINITE ELEMENT ANALYSIS

3.1 Boundary Conditions

3.1.1 Meshing

In this study, a SOLID 186 element type and a quadrilateral dominant mesh method were utilized, with an automatic approach employed for mesh generation. The number of generated elements varied depending on the thickness of the vertical axis wind turbine (VAWT) blade. Figures 1.a and 1.b show the meshing of both solid and hollow blade configurations.

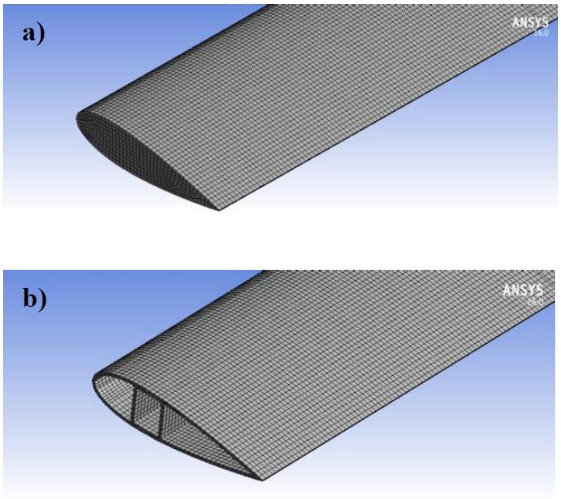

Figure 1: Meshing of the H-rotor VAWT blade: a) Solid blade, b) Hollow blade.

3.1.2 Supports

In this research, ANSYS software was employed to analyze two distinct rotor configurations with varying boundary conditions. Figure 2.a and 2.b provide details for each configuration. In the first configuration, the wind turbine blade is treated as a beam that is fixed at both ends, precisely at the aerodynamic center of the blade, situated approximately 1/4th of the chord length.

The alternative arrangement secures each blade at two positions, aligning with the Bessel points situated 20.7% from the tip of each blade. This positioning is designed to minimize the maximum bending moment, following the recommendations of multiple researchers [3, 7, 19, 21]. The calculations for this optimization are based on beam theories equations.

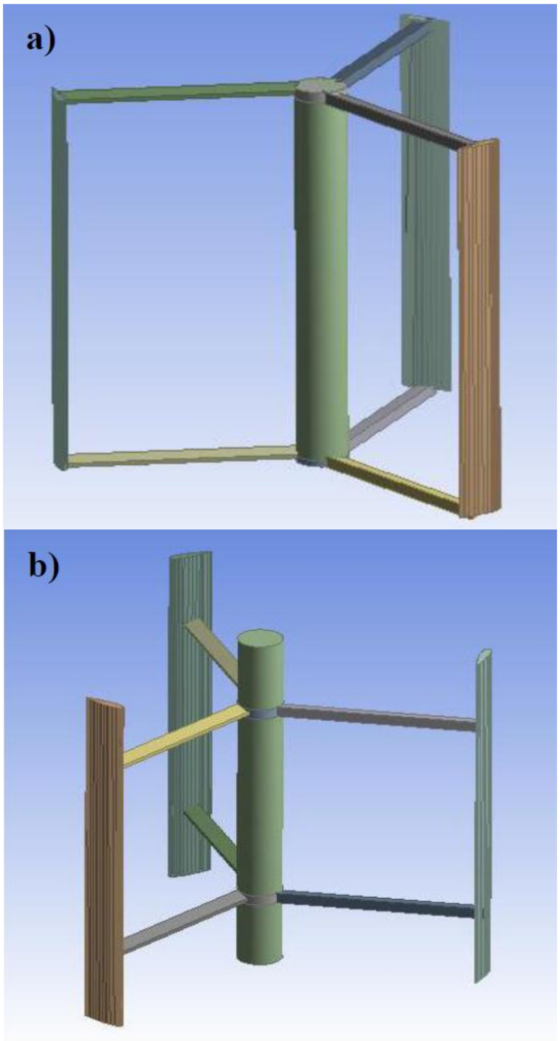

Figure 2: Supports location of the H-rotor VAWT blade a) fixed from both ends. b) fixed at the Bessel points.

3.1.3 Loads

A uniformly distributed load is applied along the surface of the VAWT blade. The main source of the load acting on the rotor blade is the radial force that is resultant of the centrifugal load and the aerodynamic load. The force distribution along the VAWT blade is given in Figure 3**.**

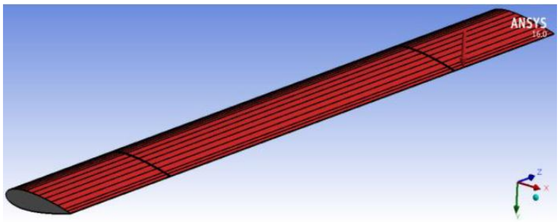

Figure 3: Uniform distributed load along the H-rotor VAWT blade.

3.2 Material Selection

The material chosen for stress analysis in the blades is an S-2 glass fiber/Epoxy Composite. Table 2 provides key mechanical and physical properties of S-2 fiberglass composites, as referenced in [22-24, 15, 25, 26].

Table 2. S-2 fiberglass properties

Property	Value
Mechanical Properties:	
Young's Modulus (GPA)	93.8
Tensile strength (MPa)	4890
Shear Modulus (GPa)	38.1
Poisson's Ratio	0.23
Elongation %	5.7
K_{IC} (MPa $m^{1/2}$)	25
Physical properties:	25
Density (gm/cm^3)	2.46

S-2 fiberglass is commonly employed in combination with high-strength epoxy resins to form efficient composite structures [22]. The material properties of carbon fiber can be found in [16]. The wind turbine blade is constructed from an S-2 fiberglass/Epoxy honeycomb composite laminate. The H-rotor VAWT blade was designed with a solid structure thickness of 42 mm, complemented by a hollow structure featuring thicknesses of 8, 7, 6, and 5 mm. The laminate structure is shown in Figure 4.

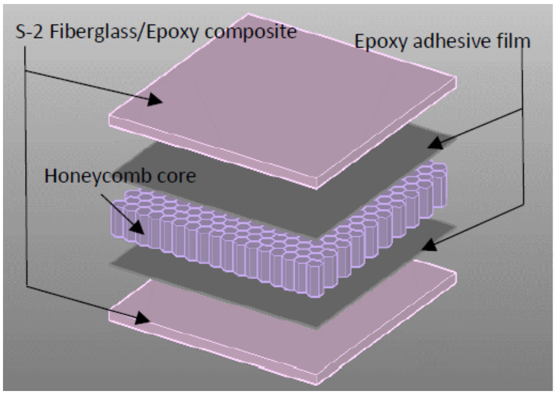

Figure 4: S-2 fiberglass / Epoxy honeycomb composite laminate.

3.3 Finite element model

The parametric definition of the finite element model relies on the chord length (C) and blade length (H). Figure 5 presents the finite element model for the first configuration.

For the second rotor configuration, the blade model underwent optimization, transitioning from a solid to a hollow cross section with a supporting strut box. Different wall thickness values were employed to mitigate weight and centrifugal forces on the blade. Throughout this analytical phase, results spanning from solid to a 5 mm wall thickness were computed under identical boundary conditions. The finite element model for the second configuration is illustrated in Figures 6.a and 6.b.

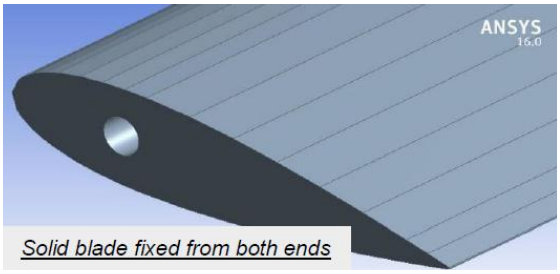

Figure 5: The finite element model for the first configuration.

4. RESULTS AND DISCUSSION

4.1 The effect of the tip speed ratio variation on the bending stress

The impact of variations in tip speed ratio on the bending stress experienced by the H-rotor VAWT blade is investigated by comparing the maximum bending stress calculated using the Engineering Theory of Beams (ETB) with that determined through FE method.

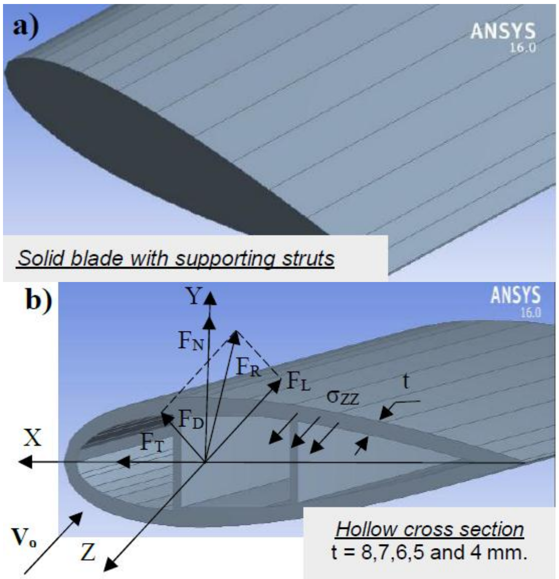

Figure 6: The second rotor configuration considered for the finite element analysis for; a) Solid blade, b) Hollow blade with different thicknesses (FD : Drag force, F_L: Lift force, F_N: Normal force ,F_T: Tangential force, FR: Resultant force, σ_{ZZ} : Bending stress, t: Blade wall thickness).

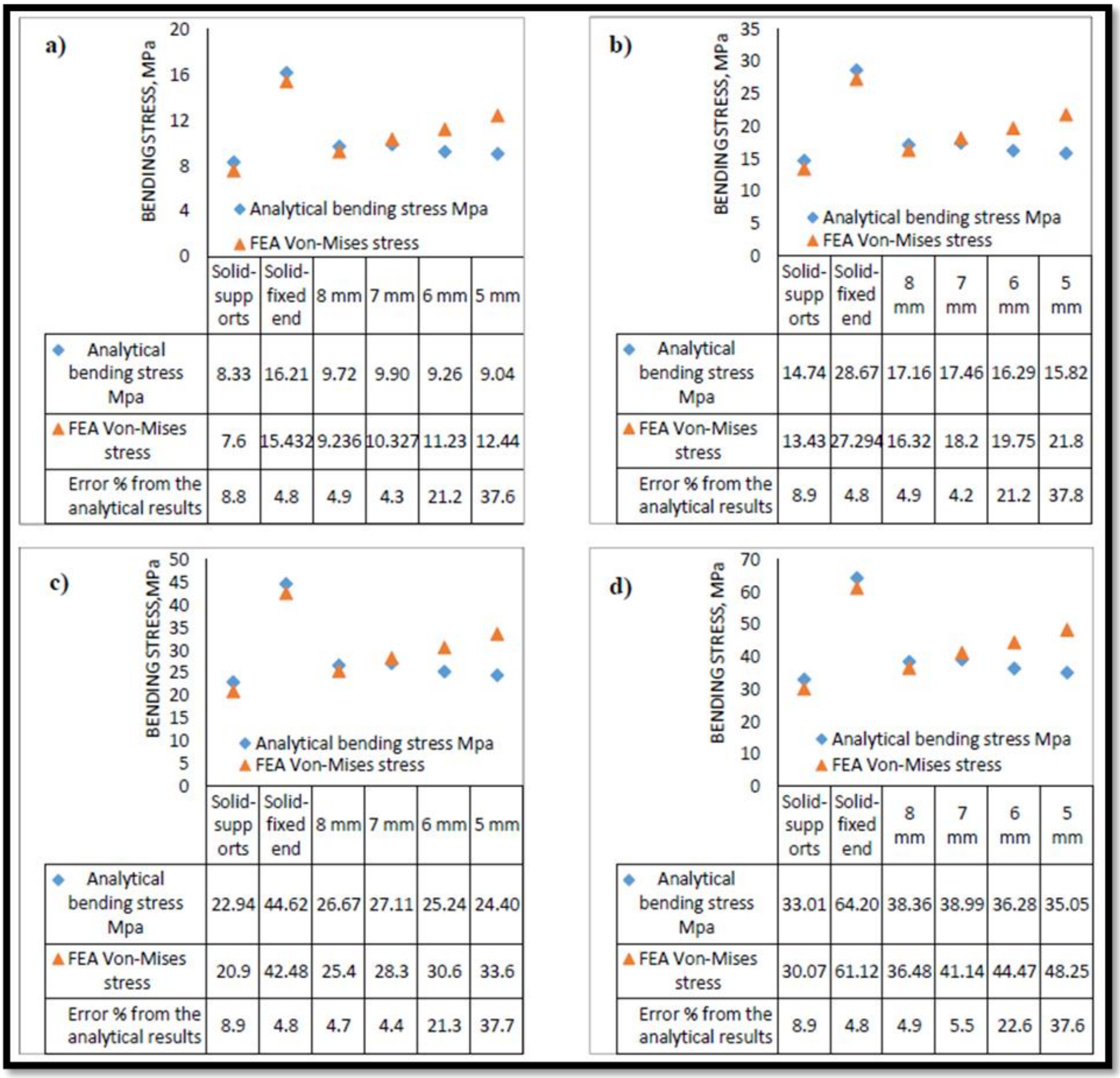

a)

	Solid-supports	Solid-fixed end	8 mm	7 mm	6 mm	5 mm
◆ Analytical bending stress Mpa	8.33	16.21	9.72	9.90	9.26	9.04
▲ FEA Von-Mises stress	7.6	15.432	9.236	10.327	11.23	12.44
Error % from the analytical results	8.8	4.8	4.9	4.3	21.2	37.6

b)

	Solid-supports	Solid-fixed end	8 mm	7 mm	6 mm	5 mm
◆ Analytical bending stress Mpa	14.74	28.67	17.16	17.46	16.29	15.82
▲ FEA Von-Mises stress	13.43	27.294	16.32	18.2	19.75	21.8
Error % from the analytical results	8.9	4.8	4.9	4.2	21.2	37.8

c)

	Solid-supports	Solid-fixed end	8 mm	7 mm	6 mm	5 mm
◆ Analytical bending stress Mpa	22.94	44.62	26.67	27.11	25.24	24.40
▲ FEA Von-Mises stress	20.9	42.48	25.4	28.3	30.6	33.6
Error % from the analytical results	8.9	4.8	4.7	4.4	21.3	37.7

d)

	Solid-supports	Solid-fixed end	8 mm	7 mm	6 mm	5 mm
◆ Analytical bending stress Mpa	33.01	64.20	38.36	38.99	36.28	35.05
▲ FEA Von-Mises stress	30.07	61.12	36.48	41.14	44.47	48.25
Error % from the analytical results	8.9	4.8	4.9	5.5	22.6	37.6

Figure 7: Comparison between the maximum bending stress calculated by the analytical and numerical methods at; a) tip speed ratio = 3, b) tip speed ratio = 4, c) tip speed ratio = 5 and d) tip speed ratio = 6.

Bending stress is computed for different blade thicknesses and for solid blades with the two rotor configurations. Figures 7.a-d illustrate the maximum bending stress values at tip speed ratios of 3, 4, 5, and 6. The percentage error between analytical and numerical calculations is provided with each figure.

Figures 7.a-d demonstrate a direct correlation between tip speed ratio and bending stress on the rotor blade. The maximum bending stress increases with higher tip speed ratios. Maintaining nearly constant wind speed and rotor dimensions while increasing the tip speed ratio leads to a rise in rotor rotational speed, resulting in increased centrifugal force acting on the rotor blade. The centrifugal force significantly influences the radial force, which is the primary source of bending stress on the blade.

4.2 Effect of the tip speed ratio variation on the maximum deflection

The determination of the maximum deflection of the rotor blade, influenced by the radial force, is illustrated in Figure 8. Calculations for maximum deflection were conducted at tip speed ratios of 3, 4, 5, and 6.

It is evident that the maximum deflection rises with an increase in tip speed ratio, attributed to the increase of the bending stress on the rotor blade.

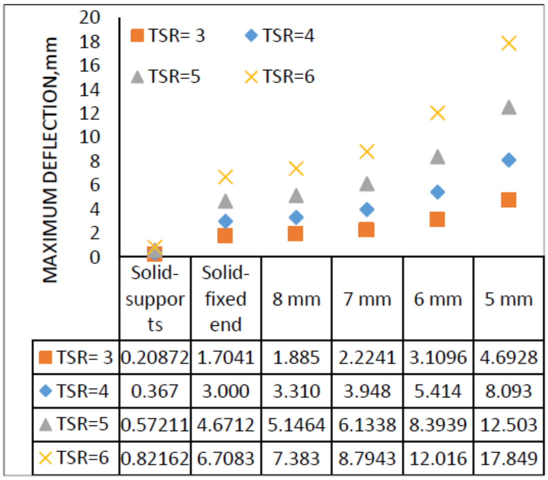

	Solid-supports	Solid-fixed end	8 mm	7 mm	6 mm	5 mm
■ TSR= 3	0.20872	1.7041	1.885	2.2241	3.1096	4.6928
◆ TSR=4	0.367	3.000	3.310	3.948	5.414	8.093
▲ TSR=5	0.57211	4.6712	5.1464	6.1338	8.3939	12.503
× TSR=6	0.82162	6.7083	7.383	8.7943	12.016	17.849

Figure 8: Variation between the maximum deflection values for different VAWT H-rotor blade thicknesses at tip speed ratio = 3, 4, 5 and 6.

4.3 Bending stress variation with the azimuth angle

Ensuring the stability of the VAWT blade structure is imperative under both static and dynamic load conditions. The rotation of VAWT blades, experiencing a complete 360^{o} dynamic load cycle, induces stress variations along the blade azimuth angle, leading to fatigue loads on the VAWT blades.

Figure 9.a depicts the variation of bending stress along the blade azimuth angle for different blade thicknesses, highlighting the variation of the stress distribution.

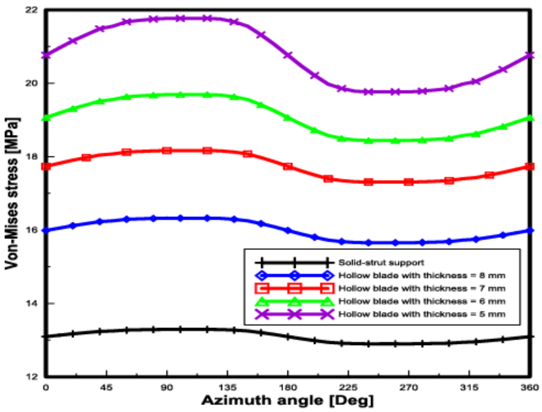

Figure 9 a) Relationship between the Von-Mises stress and the azimuth angle for different H-rotor blade thicknesses at tip speed ratio = 4 using S-2 fiberglass/epoxy composite.

For a clearer representation of the bending stress variation along the blade azimuth angle, Figure 9.b presents the relationship between Von-Mises stress and the blade azimuth angle for a solid H-rotor blade with strut supports at a tip speed ratio of 4.

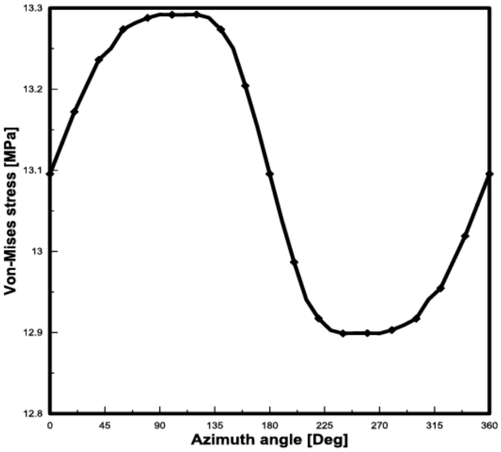

Figure 9 b) Relationship between the Von-Mises stress and the azimuth angle for solid H-rotor blade cross section with strut supports at tip speed ratio = 4.

4.4 S-2 Fiberglass composites versus carbon fiber composites

4.4.1 Maximum bending stress

S-2 fiberglass composites exhibit numerous favorable mechanical properties, making them suitable for use in designing H-rotor VAWT blades. However, carbon fiber composites are also commonly employed in the manufacturing of wind turbine blades. A comparative analysis was conducted, examining the maximum bending stress and maximum deflection when utilizing these two composite laminates.

The maximum bending stress values at tip speed ratios of 3, 4, 5, and 6 for the S-2 fiberglass carbon fiber composite laminate are illustrated in Figures 10.a-d.

Figures 10.a-d demonstrate that, across various tip speed ratios, carbon fiber composites yield higher maximum bending stress values acting on the wind turbine blade.

4.4.2 Maximum deflection

To facilitate the comparison between S-2 fiberglass and carbon fiber composite laminates, the maximum deflection of the rotor blade was calculated for both materials. Results are presented in Figures 11.a-d for tip speed ratios of 3, 4, 5, and 6.

The maximum deflection values are closely aligned in the solid blade with the two rotor configurations when utilizing S-2 fiberglass and carbon fiber composite laminates. However, in the case of the hollow blade, carbon fiber composites induce higher deflections in the rotor blade compared to S-2 fiberglass composites across all analyzed tip speed ratios.

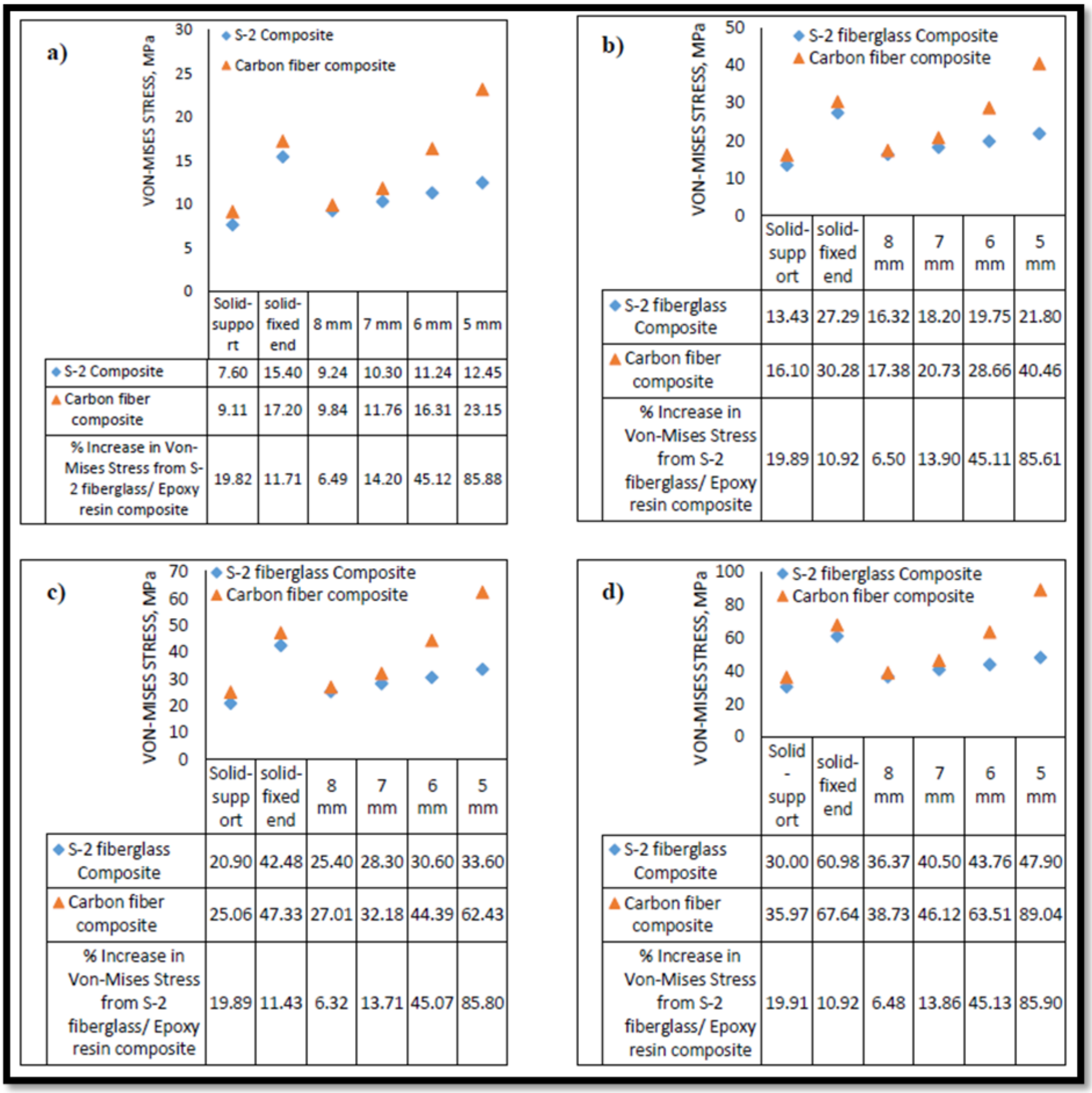

a)

	Solid-support	solid-fixed end	8 mm	7 mm	6 mm	5 mm
◆ S-2 Composite	7.60	15.40	9.24	10.30	11.24	12.45
▲ Carbon fiber composite	9.11	17.20	9.84	11.76	16.31	23.15
% Increase in Von-Mises Stress from S-2 fiberglass/ Epoxy resin composite	19.82	11.71	6.49	14.20	45.12	85.88

b)

	Solid-support	solid-fixed end	8 mm	7 mm	6 mm	5 mm
◆ S-2 fiberglass Composite	13.43	27.29	16.32	18.20	19.75	21.80
▲ Carbon fiber composite	16.10	30.28	17.38	20.73	28.66	40.46
% Increase in Von-Mises Stress from S-2 fiberglass/ Epoxy resin composite	19.89	10.92	6.50	13.90	45.11	85.61

c)

	Solid-support	solid-fixed end	8 mm	7 mm	6 mm	5 mm
◆ S-2 fiberglass Composite	20.90	42.48	25.40	28.30	30.60	33.60
▲ Carbon fiber composite	25.06	47.33	27.01	32.18	44.39	62.43
% Increase in Von-Mises Stress from S-2 fiberglass/ Epoxy resin composite	19.89	11.43	6.32	13.71	45.07	85.80

d)

	Solid-support	solid-fixed end	8 mm	7 mm	6 mm	5 mm
◆ S-2 fiberglass Composite	30.00	60.98	36.37	40.50	43.76	47.90
▲ Carbon fiber composite	35.97	67.64	38.73	46.12	63.51	89.04
% Increase in Von-Mises Stress from S-2 fiberglass/ Epoxy resin composite	19.91	10.92	6.48	13.86	45.13	85.90

Figure 10: Comparison between the maximum equivalent Von-Mises stresses values when using S-2 fiberglass/Epoxy and Carbon fiber/Epoxy composite for different VAWT H-rotor blade cross sections at; a) tip speed ratio = 3, b) tip speed ratio = 4, c) tip speed ratio = 5 and d) tip speed ratio = 6.

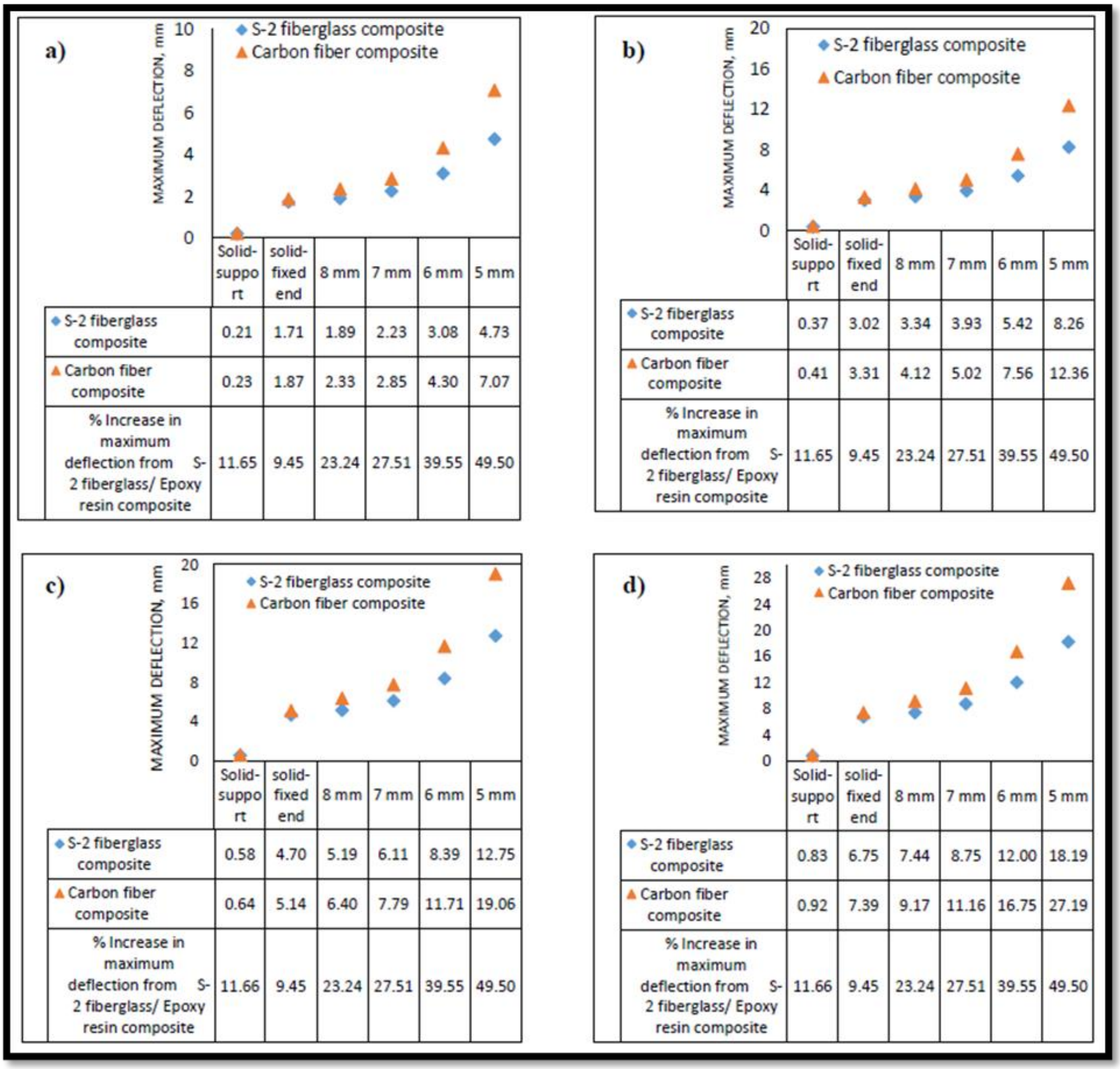

a)

	Solid-support	solid-fixed end	8 mm	7 mm	6 mm	5 mm
◆ S-2 fiberglass composite	0.21	1.71	1.89	2.23	3.08	4.73
▲ Carbon fiber composite	0.23	1.87	2.33	2.85	4.30	7.07
% Increase in maximum deflection from S-2 fiberglass/ Epoxy resin composite	11.65	9.45	23.24	27.51	39.55	49.50

b)

	Solid-support	solid-fixed end	8 mm	7 mm	6 mm	5 mm
◆ S-2 fiberglass composite	0.37	3.02	3.34	3.93	5.42	8.26
▲ Carbon fiber composite	0.41	3.31	4.12	5.02	7.56	12.36
% Increase in maximum deflection from S-2 fiberglass/ Epoxy resin composite	11.65	9.45	23.24	27.51	39.55	49.50

c)

	Solid-support	solid-fixed end	8 mm	7 mm	6 mm	5 mm
◆ S-2 fiberglass composite	0.58	4.70	5.19	6.11	8.39	12.75
▲ Carbon fiber composite	0.64	5.14	6.40	7.79	11.71	19.06
% Increase in maximum deflection from S-2 fiberglass/ Epoxy resin composite	11.66	9.45	23.24	27.51	39.55	49.50

d)

	Solid-support	solid-fixed end	8 mm	7 mm	6 mm	5 mm
◆ S-2 fiberglass composite	0.83	6.75	7.44	8.75	12.00	18.19
▲ Carbon fiber composite	0.92	7.39	9.17	11.16	16.75	27.19
% Increase in maximum deflection from S-2 fiberglass/ Epoxy resin composite	11.66	9.45	23.24	27.51	39.55	49.50

Figure 11 : Comparison between the maximum deflection [mm] values when using S-2 fiberglass/epoxy and carbon fiber/epoxy composite for different VAWT H-rotor blade cross sections at; a) tip speed ratio = 3, b) tip speed ratio = 4, c) tip speed ratio = 5 and d) tip speed ratio = 6.

5. CONCLUSIONS

The study's findings yield the following noteworthy observations:

1- Optimal conditions for maximum bending stress in rotor blades are achieved when they are fixed at both ends.
2- Implementing blade attachment at the Bessel points of the rotor struts effectively mitigates bending stress exerted on the rotor blades.
3- The bending stress experienced by the rotor blades is directly influenced by the tip speed ratio, showing higher values as the tip speed ratio increases.
4- Increased tip speed ratios correlate with augmented maximum deflection in rotor blades.
5- The utilization of carbon fiber composites in rotor blades induces greater deflection compared to S-2 fiberglass blades, signifying the material's impact on rotor blade behavior.

In conclusion, the study highlights the importance of proper blade attachment and tip speed ratio optimization in minimizing bending stress and deflection and hence the structural integrity in rotor blades. Additionally, the choice of materials, such as S-2 fiberglass composites, can significantly impact the structural behavior of the blades in terms of deflections and stresses.

Author contribution:
Rasha M. Soliman: Methodology, Verification, Formal analysis, and writing original draft, Investigation. ***Shaban M. Abdo***: Methodology, Writing-review and editing, and Supervision. ***Aly El Domiaty***: Idea of the research point, Investigation, and Supervision. ***Mohamed Lotfy:*** Investigation, Methodology, Verification, Editing, and Supervision. All authors have read and agreed to the published version of the manuscript.

Competing interests: The authors declare there are no competing interests.

Funding: The authors declare no specific funding for this work.

6. REFERENCES

[1] Lee, Y., "Numerical Study Of The Aerodynamic Performance of a 500 W Darrieus-Type Vertical-Axis Wind Turbine," Renewable Energy, Vol. 83, pp. 407-415, 2015.

[2] Spera, D.A., "Introduction to Modern Wind Turbines," in Wind Turbine Technology: Fundamental Concepts in Wind Turbine Engineering, Second Edition, Editor: D.A. Spera, ASME Press, 2009.

[3] Castillo, J., "Small-Scale Vertical Axis Wind Turbine Design," Bachelor’s thesis, Tampere University of Applied Sciences, Aeronautical Engineering, Tampere, Finland, 2011.

[4] Rossander, M., Dyachuk, E., Apelfröjd, S., Trolin, K. , Goude, A., Bernhoff, H., Eriksson , S., "Evaluation of a Blade Force Measurement System for a Vertical Axis Wind Turbine Using Load Cells ", Energies, 8(6) 5973-5996, 2015.

[5] Dyachuk, E., Rossander,M., Goude,A., Bernhoff, H., "Measurements of the Aerodynamic Normal Forces on a 12-kW Straight-Bladed Vertical Axis Wind Turbine, " Energies, 8(8), 8482-8496, 2015.

[6] Vrian Hand, and Andrew Cashman, “A review on the historical development of the lift-type vertical axis wind turbine: From onshore to offshore floating application”, Sustainable Energy Technologies and Assessments, Vol. 38, April 2020.

[7] Hameed, M.S. and Afaq, S.K., "Design And Analysis of A Straight Bladed Vertical Axis Wind Turbine Blade Using Analytical And Numerical Techniques," Ocean Engineering, Vol. 57, pp. 248-255, 2013.

[8] H. Nezzar, F. Ferroudji, T. Outtas, L. Saihi, K. Roummani, K. Koussa, D. Boukhlef, “Modelling and Stress Analysis of an Aluminum Blade for Vertical Axis Wind Turbine”, 2nd International Conference on Advanced Electrical Engineering (ICAEEE), October 29th-31st , 2022.

[9] Rahman M., S.A., Freeman A., Denham J., Christopher L., Huggins W., Johnson Z., and Ragland J., "Finite Element Modeling of Structural Design Optimization of Various Vertical Axis Wind Turbine Models," HEFAT2014 10th International Conference on Heat Transfer, Fluid Mechanics and Thermodynamics, Orlando, Florida, 14-16 July, 2014.

[10] Liu, W. and Xiao, Q., "Investigation on Darrieus Type Straight Blade Vertical Axis Wind Turbine with Flexible Blade," Ocean Engineering, 110(3-4), pp. 339-356, 2015.

[11] Yutaka Hara, Naoki Horita, Shigeo Yoshida, Hiromichi Akimoto, and Takahiro Sumi, “Numerical Analysis of Effects of Arms with Different Cross-Sections on Straight-Bladed Vertical Axis Wind Turbine”, Energies, Vol. 12, Issue 11, June 2019.

[12] Yanzhao Yang, Zhiping Guo, Qing Song, Yanfeng Zhang, and Qing’an Li, “Effect of Blade Pitch Angle on the Aerodynamic Characteristics of a Straight-bladed Vertical Axis Wind Turbine Based on Experiments and Simulations,” Energies, Vol. 11, Issue 6, June 2018.

[13] Brian Hand, Ger Kelly, Andrew Cashman, “Structural analysis of an offshore vertical axis wind turbine composite blade experiencing an extreme wind load”, Marine Structures, Vol. 75, Jan 2021.

[14] Prince Arora, Prashant Parmeshwar Atkale, Badri Prasad Patel, Suhail Ahmad, “Response Analysis of Composite Blades of Offshore VAWT Using CFD and FSI for the Indian Ocean”, International Conference on Offshore Mechanics and Arctic Engineering, Sep. 22nd, 2023.

[15] Soliman, R., Lotfy ,M., Abdou ,S. , El Domiaty, A., "Aerodynamic Loads On A 3-Bladed H-Rotor Vertical Axis Wind Turbine: Parametric Study And Experimental Validation", Port Said Engineering Research Journal, Vol. 21, No. 2, Sep. 2017.

[16] Soliman, R., “Fracture Behavior Of Joints Manufactured From Composite Materials,” Ph.D. Dissertation, Production Engineering and Mechanical Design Dept., Faculty of Engineering, Port Said University, 2017.

[17] Paraschivoiu, I., "Wind Turbine Design with Emphasis on Darrieus Concept," Internationales Polytechnique, 2002.

[18] Kirke, B.K., "Evaluation of Self-Starting Vertical Axis Wind Turbines for Stand-Alone Applications," Ph.D., Griffith University, Australia, 1998.

[19] Islam, M., Fartaj,A., and Carriveau, R., "Analysis of the Design Parameters Related to a Fixed-Pitch

Straight-Bladed Vertical Axis Wind Turbine," Wind Engineering, Vo. 32, issue 5, 2008.

[20] Perkins, F. and Cromack, D., "Wind Turbine Blade Stress Analysis And Natural Frequencies," Wind Energy Center Reports 11, United States, 1978.

[21] Ade, N. and Mone,T., "Vertical Axis Wind Turbine Designed To Utilize Turbulence Created by Frequently Passing Trains," International Journal of Scientific & Engineering Research, Vol.5, Issue 5, 2014.

[22] Shukla,A. , Grogan, J., Tekalur,S., Bogdanovich , A. and Coffelt, R., "Ballistic Resistance of 2d & 3d Woven Sandwich Composites," Composites Properties and Applications: Proceedings of the Ninth International Conference on Composite Materials (ICCM/9), Madrid, 2005.

[23] Wallenberger, F. T., "Fiberglass and Glass Technology: Energy-Friendly Compositions and Applications," Springer Science & Business Media, Editors: Frederick T. Wallenberger, Paul A. Bingham, 2009.

[24] Burrill, D., and Zurschmeide, J., "How to Fabricate Automotive Fiberglass & Carbon Fiber Parts," CarTech Inc., Publsiher: S-A Design, 2012.

[25] TAP Plastics, Available from: https://www.tapplastics.com, 2017.

[26] Thermostatic Industries, Available from: http://www.thermostatic.com, 2017.